

Haze and Its Impact to Paddy Monitoring from Remote Sensing Satellites

Asmala Ahmad¹, Hamzah Sakidin², Agus Dahlia³, Zetriuslita³, Rahma Qudsi³

¹Centre for Advanced Computing Technology (C-ACT), Fakulti Teknologi Maklumat Dan Komunikasi (FTMK), Universiti Teknikal Malaysia Melaka (UTeM), Melaka, MALAYSIA, asmala@utem.edu.my

²Department of Fundamental and Applied Sciences, Universiti Teknologi PETRONAS, Perak, MALAYSIA, hamzah.sakidin@utp.edu.my

³Program Studi Pendidikan Matematika FKIP Universitas Islam Riau, INDONESIA, zetriuslita@edu.uir.ac.id

ABSTRACT

Haze is a common phenomenon in Malaysia and is caused by smoke which originates from forest fires in neighbouring countries. It causes visibility to drop, therefore affecting agricultural monitoring from remote sensing satellites. Such scenarios have caused problems in monitoring crops particularly those having short growth duration such as paddy. This study aims to investigate the haze scenarios in Malaysia and its impact on paddy monitoring from remote sensing satellites. The study makes use of visibility data and Landsat satellite imagery over Malaysia from 1999 to 2008. The result shows that within this period, the 2008 planting season was the most affected by haze where 9 out of 10 satellite overpasses occurred during the conditions where visibility was 10 km or less.

Key words: Haze, paddy, remote sensing, satellite, visibility.

1. INTRODUCTION

Haze is partially opaque condition of the atmosphere caused by tiny suspended solid or liquid particles in the lower atmosphere [1]. Haze reduces visibility due to the attenuation caused by scattering and absorption of solar radiation by haze constituents [2]. Haze consists of suspension of fine solid particles or liquid droplets, and trace gases. Studies have shown that haze which originates from biomass burning contains large amounts of hazardous gases, i.e., carbon monoxide (CO), nitrogen dioxide (NO₂) and sulphur dioxide (SO₂), and particulate matter, i.e., PM₁₀ [3].

The thick haze that occurs in Malaysia is caused mainly by smoke originating from large forest fires in Indonesia, due to agricultural clean-up activities as farmers and large companies convert forests into plantations using fire to clear land [4]. Major forest fires occurred in 1982, 1983, 1987, 1991, 1994, 1997, 1998, 2002, 2004, 2005, 2010 and 2013.

Haze occurrences have also been reported in other parts of the world such as Africa and South America. In South America, plumes and haze layers originate from biomass burning that occurs every year over the central Amazon Basin due mainly to deforestation and land conversion [5]. The haze layers occur at altitudes between 1000 and 4000 m and are 100 to 300 m thick but extend horizontally over several hundred kilometres. The emissions from the burning significantly affect the chemical and optical characteristics of the atmosphere over the Amazon Basin [6].

In West Africa, during the dry season, biomass burning occurs particularly in the Sahelian regions, due to the burning of agricultural waste [7]. Emissions from these fires were reported to reach as far as South Africa. The Southern African Regional Science Initiative [8] studied the generation, transport, and deposition of the associated aerosols to develop better understanding of related environmental processes, such as the effect of haze on the global radiation balance.

1.1 Atmospheric Scattering and Absorption

Atmospheric scattering and absorption depend very much on the wavelength of the radiation and the size of the atmospheric constituents it interacts with. Scattering is much stronger for short wavelengths than long wavelengths. Particles with size approximately 0.1 to 10 μm are particularly effective in Mie scattering in the visible wavelength regions (0.4 – 0.7 μm) hence can impair ground level visibilities. To define visibility, the fraction of light intensity reaching the observer can be expressed as [9]:

$$\frac{I_{obs}}{I_0} = \exp \left[- \int_0^{X_{obs}} b_{ext}(x) dx \right] \quad (1)$$

where x is distance from observer, I_0 is the original intensity of an object, I_{obs} is the intensity reaching the observer, and

is the extinction coefficient evaluated at 0.55 μm wavelength, assumed to be horizontally uniform.

The visibility is defined as the value of X_{obs} . The fraction on the left at which the contrast between an object and its background can no longer be distinguished is often approximated by 0.02 [9]. Hence:

$$0.02 = \exp \left[- \int_0^{X_{obs}} b_{ext}(x) dx \right] \tag{2}$$

$$0.02 = \exp(-b_{ext}x|_0^{X_{obs}}) \tag{3}$$

$$\ln(0.02) = -b_{ext}x_{obs} \tag{4}$$

Hence,

$$visibility = - \frac{\ln(0.02)}{b_{ext}} \tag{5}$$

This is known as the Koschmieder equation and is used to define visibility. Visibility is inversely proportional to the extinction coefficient, which can be related to atmospheric aerosol concentrations [10]. b_{ext} represents the extinction coefficient for 1 km thickness, which is relevant to the whole vertical haze loading [11], and is therefore equivalent to the corresponding aerosol optical thickness. depends on the presence of gases and molecules that scatter and absorb light in the atmosphere and is given by [9]:

$$b_{ext} = b_{ray} + b_{mie} + b_{ns} + b_{abs} \tag{6}$$

where b_{ray} is Rayleigh scattering by gaseous molecules, b_{mie} is Mie scattering by particles, b_{ns} is non-selective scattering caused by bigger particles and b_{abs} is absorption by gaseous molecules. These various extinction components are functions of wavelength.

In most cases, particle scattering controls visibility reduction [9]. Figure 1 illustrates the scattering and absorption efficiency per unit volume as a function of particle diameter and shows the predominance of scattering over absorption at 550 nm wavelength. It also signifies that most scattering is caused by particles with diameters 0.1 – 1.0 μm, which are within the PM₁₀ category [9]. Visibility reduction associated with forest fires is due to scattering by particles (i.e. PM₁₀) and to a lesser extent, absorption of light by trace gases with diameters of approximately 5 x 10⁻⁴ μm (i.e. NO₂, SO₂, and CO) [2]. The definition for clear sky visibility varies, but is normally considered to be 20 to 23 km [12].

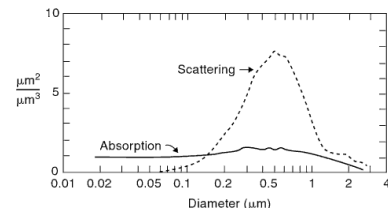


Figure 1: Scattering and absorption cross section per unit volume as a function of particle diameter [9]

1.2 Haze Monitoring in Malaysia

In Malaysia, haze monitoring is carried out by the Malaysian Meteorological Department and Department of Environment Malaysia in terms of visibility and air pollution index (API) respectively. Visibility measurement is carried out by the Malaysian Meteorological Department daily through a network of 149 monitoring stations. For public convenience, haze severity is categorised into five levels; visibilities more than 10 km represent ‘clear’, 5 to 10 km visibilities represent ‘moderate’, 2 to 5 km visibilities represent ‘hazy’, 0.5 to 2 km visibilities represent ‘very hazy’ and visibilities less than 0.5 km represent ‘extremely hazy’ (Table 1).

Table 1: Visibility levels used by the Malaysian Meteorological Department

Severity	Horizontal Visibility (km)
Clear	> 10
Moderate	5 – 10
Hazy	2 – 5
Very hazy	0.5 – 2
Extremely hazy	< 0.5

The Department of Environment Malaysia operates a network of 51 stations, where 36 stations are in West Malaysia (or Peninsular Malaysia) and 15 in East Malaysia. Figure 2 shows the location of air quality monitoring stations in West Malaysia and a typical monitoring station [14]. Due to the potential harm to human health, five main pollutants measured by the Department of Environment are SO₂, NO₂, CO, O₃ and PM₁₀. Based on their locations and the types of pollutant measured, the stations are categorised into five categories: Residential (20 stations), Industrial (12 stations), Traffic (1 station), Background (1 station) and PM₁₀ (2 stations). The difference between these categories is the types of pollutant measured (Table 2).

Table 2: Station categories and the type of pollutants measured [13]

Category	SO ₂	NO ₂	CO	O ₃	PM ₁₀
Industrial	X	X	-	-	X
Residential	X	X	X	X	X
Traffic	X	X	-	X	X
Background	X	X	X	X	X
PM ₁₀	-	-	-	-	X

In the API system, the air quality levels are categorised into: good (0 – 50), moderate (51 – 100), unhealthy (101 – 200), very unhealthy (201 – 300), hazardous (300 – 500) and emergency (> 500) (Table 3). The API value reported for a given time period represents the highest API value among all pollutants during that particular time period; the predominant pollutant during haze episodes is PM₁₀[2].



Figure 2: Location of air quality monitoring stations in West Malaysia (left) with an enlarged version of Selangor state (lower left sub-section) and a typical monitoring station (right)

The Recommended Malaysian Air Quality Guidelines forms the basis for calculating the API and consists of two key aspects: the averaging time and the Malaysian guidelines (Table 4). The averaging time differs for different air pollutants and represents the period of time over which the measurements are made and recorded in running averages. For reporting purposes, the same averaging times are used: PM₁₀ and SO₂ (24-hour running averages), CO (8-hour running averages), and O₃ and NO₂ (1-hour running averages) [15]. The Malaysian guidelines represent the safe level for each pollutant and were derived based on human health data and recommendations from the World Health Organisation (WHO). For example, a PM₁₀ concentration of 150 µg/m³ corresponds to 100 API and is the upper limit for the safe level; PM₁₀ concentrations exceeding this are likely to cause adverse health effects [15]. Conversion of the PM₁₀ concentration from µg/m³ to API can be done using the equations shown in Table 5. Malaysia has a typical tropical monsoon climate characterized by uniformly high mean temperature (approximately 27°C), with a relatively high mean annual rainfall (exceeding 2000 mm per year) and humidity (70% - 90%) throughout the year. The wind over the country is generally mild and variable. However, there are some periodic changes in the wind flow patterns that describe

the two monsoon seasons namely the North-east Monsoon, known as the wet season (November to March) and the Southwest Monsoon, known as the dry season (June to September). The remaining months i.e. April to May and October to November are known as the transitional periods. Because the wind comes from the south-west and there is much less rain during the Southwest Monsoon and the second transitional period, smoke from the forest fires in Sumatra remains suspended in the atmosphere for a long time and drifts to Malaysia, causing haze.

Table 3: API status, level of pollution and health measures [15]

API	Status	Level of Pollution	Health Measure
0 – 50	Good	Low, no ill effects on health.	No restriction of activities to all groups.
51 – 100	Moderate	Moderate, no ill effects on health.	No restriction of activities to all groups.
101 – 200	Unhealthy	Mild aggravation of symptoms and decreased exercise tolerance in persons with heart or lung disease.	Restriction of outdoor activities for high-risk persons. General population should reduce vigorous outdoor activity.
201 – 300	Very Unhealthy	Significant aggravation of symptoms and decreased exercise tolerance in persons with heart or lung disease.	Elderly and persons with known heart or lung disease should stay indoors and reduce physical activity. General population should reduce vigorous outdoor activity. Those with any health problems to consult doctor
300 – 500	Hazardous	Severe aggravation of symptoms and endangers health.	Elderly and persons with existing heart or lung disease should stay indoors and reduce physical activity. General population should reduce vigorous outdoor activity.
> 500	Emergency	Severe aggravation of symptoms and endangers health.	General population advised to follow the orders of National Security Council and always follow announcements through the mass media.

Table 4: Air quality measurement guidelines [15]

Pollutant	Averaging Time	Malaysian Guidelines	
		(ppm)	($\mu\text{g}\text{m}^{-3}$)
O ₃	1 hour	0.10	200
	8 hours	0.06	120
CO	1 hour	30	35
	8 hours	9	10
NO ₂	1 hour	0.17	320
	24 hours	0.04	-
SO ₂	1 hour	0.13	350
	24 hours	0.04	105
PM ₁₀	24 hour	N/A	150
	1 year		50

Table 5: Equations for API calculation based on PM₁₀ 24-hour running averages [15]

PM ₁₀ concentration, C ($\mu\text{g}\text{m}^{-3}$)	Equation used for conversion to API
$C \leq 50$	$API = C$
$50 < C \leq 350$	$API = 50 + [(C - 50) \times 0.5]$
$350 < C \leq 420$	$API = 200 + [(C - 350) \times 1.43]$
$420 < C \leq 500$	$API = 300 + [(C - 420) \times 1.25]$
$C \geq 500$	$API = 400 + (C - 500)$

During the 2005 haze episode, the haze caused a drop in visibility in most places in Malaysia. Figure 3 shows photos of clear and hazy conditions in Putrajaya, the federal administrative centre of Malaysia, located about 30 km from Kuala Lumpur. Figure 4 shows location of Malaysia and map of Malaysia while Figure 5 shows the haze condition on August 10, 2005, with active fires from August 5 to 12, 2005, observed by MODIS and the Southeast Monsoon wind pattern on August 10, 2005. Due to the hazardous properties of the haze constituents, a sudden increase in respiratory and eye-related illnesses cases was reported. The drop in visibility conditions also badly affected economy-related activities including tourism, transportation, fisheries and production sectors, which caused a big loss to Malaysia.

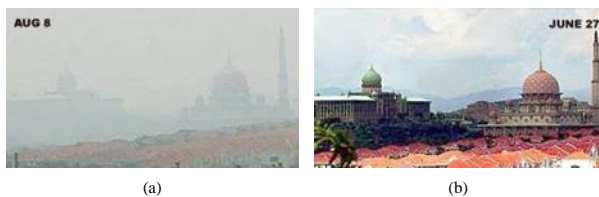


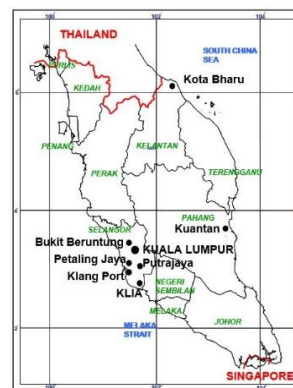
Figure 3: The Prime Minister’s Department (left building) and the Putra Mosque (right building) in Putrajaya, the federal administrative centre of Malaysia during (a) hazy (8 August 2005) and (b) clear (27 June 2005) [17]

2. MATERIALS AND METHODS

In this study, API data were obtained from the Department of Environment Malaysia for the several areas in Malaysia, i.e. Klang Port, Petaling Jaya, Kuantan and Kota Bharu for 2005. The satellite images used are from Landsat satellite supported by NOAA (National Oceanic and Atmospheric Administration) and TOMS-EP (Total Ozone Mapping Spectrometer-Earth Probe) satellite. Initially, API data for Klang Port, Petaling Jaya, Kuantan and Kota Bharu were analysed through a graph where daily visibility and PM₁₀ intensity were plotted. Colour horizontal boundary was drawn based on visibility. White, yellow, green, violet and red colours indicate clear (above 10 km), moderate (5 – 10 km), hazy (2 – 5 km), very hazy (0.5 – 2 km) and extremely hazy (less than 0.5 km). Next, the visibility for two different locations were plotted in a scatter plot to investigate their correlation. This involved Petaling Jaya versus Klang Port, Petaling Jaya versus Kuantan and Petaling Jaya versus Kota Bharu dan Kuantan versus Kota Bharu. Subsequently, further analysis was carried out by integrating satellite images with visibility data. Finally, the impact of haze was investigated by considering precision farming of paddy as a case study.



(a)



(b)

Figure 4: (a) Location of Malaysia and (b) Map of Malaysia

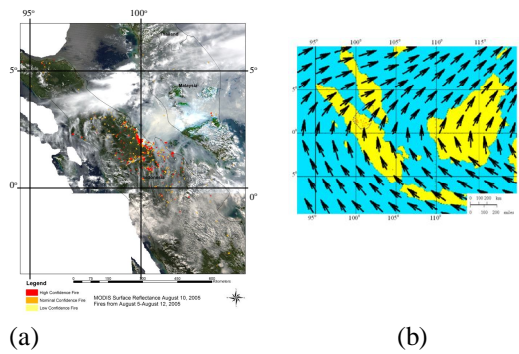


Figure 5: (a) The haze condition on August 10, 2005, with active fires from August 5 to 12, 2005, observed by MODIS; masked in white are mostly ocean areas [16] and (b) the Southeast Monsoon wind pattern on August 10, 2005 [17]

3. RESULTS AND DISCUSSION

Figure 6 shows visibility and PM₁₀ intensity against Landsat overpass date in 2005 for Klang Port, Petaling Jaya, Kuantan and Kota Bharu. The sudden increase in PM₁₀ and drop in visibility in August 2005, particularly in Klang Port and Petaling Jaya, is associated with the occurrence of haze in that year. Extreme haze occurred between 6 and 22 August 2005. Klang Port and Petaling Jaya, which are located on the west of Malaysia, with average visibility and PM₁₀ concentration approximately 11 km and 70 API respectively. These places experienced lower visibility and higher PM₁₀ intensity than Kuantan and Kota Bharu, with average visibility and intensity approximately 14 km and 40 API respectively, which are located on the east. Since extremely hazy and very hazy conditions are quite rare in Malaysia, we are more concerned on a more frequently occurring conditions.

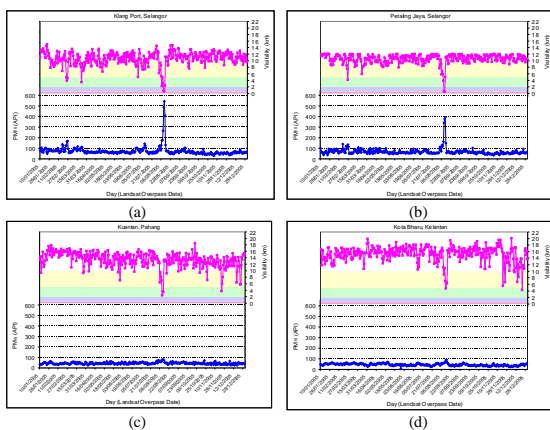


Figure 6: Visibility and PM₁₀ intensity for (a) Klang Port, (b) Petaling Jaya, (c) Kuantan and (d) Kota Bharu stations. White, yellow, green, violet and red colours indicate clear (above 10 km), moderate (5 – 10 km), hazy (2 – 5 km), very hazy (0.5 – 2 km) and extremely hazy (less than 0.5 km) conditions respectively

Figure 7 shows scatterplots of visibility for Petaling Jaya vs. Klang port, Petaling Jaya vs. Kuantan, Petaling Jaya vs. Kota Bharu and Kuantan vs. Kota Bharu, together with linear fits to these plots. It is clear that the visibility correlation between nearby stations, i.e. Petaling Jaya and Klang Port (0.708) is much higher than non-neighbouring stations, that are Petaling Jaya and Kuantan (0.04), Petaling Jaya and Kota Bharu (0.02) and Kuantan and Kota Bharu (0.08). Hot spot distributions of forest fire in Indonesia from 6 and 10 August 2005 are shown in Figure 8. On 6 August 2005, hot spots scattered at several locations in Sumatra and Kalimantan. On 10 August 2005, there seems to be an increased number of hot spots in Sumatra.

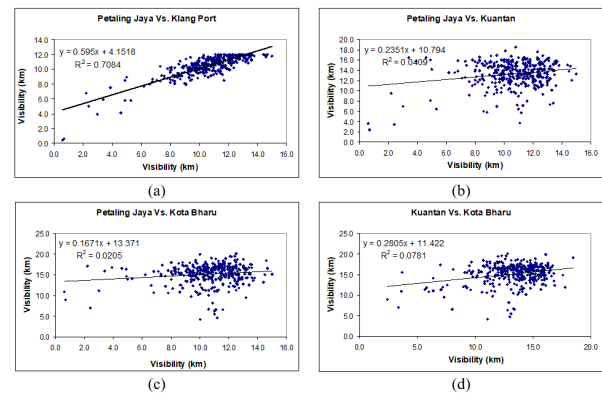


Figure 7: Visibility correlation for (a) Petaling Jaya vs. Klang port, (b) Petaling Jaya vs. Kuantan, (c) Petaling Jaya vs. Kota Bharu and (d) Kuantan vs. Kota Bharu

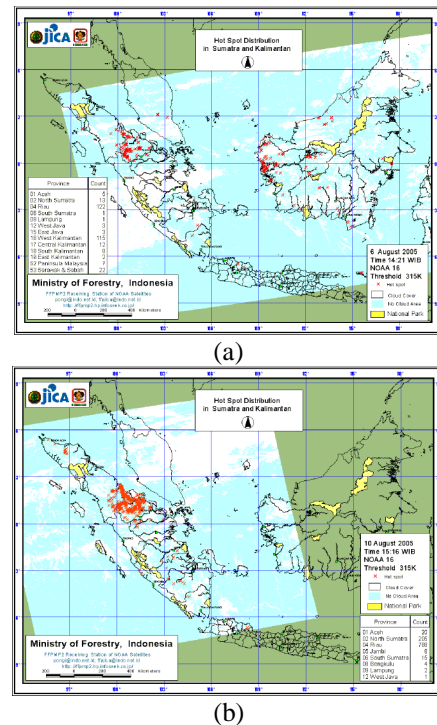


Figure 8: Fire distributions on (a) 6 and (b) 10 August 2005 determined from NOAA 16 satellite [19]

These forest fires release a huge amount of smoke that contains particulates and gases into the atmosphere [2]. The smoke is carried by the Southwest Monsoon wind to neighbouring countries, such as Malaysia, Singapore, Thailand and Brunei, and can travel hundreds of kilometres across the Southeast Asian region, reaching the Philippines. Haze conditions over Malaysia and Indonesia, based on the aerosol index measured using the Total Ozone Mapping Spectrometer (TOMS) from 10 and 11 August 2005 are shown in Figure 9. These are extreme examples, but lower level haze is a common occurrence, as seen in Figure 10.

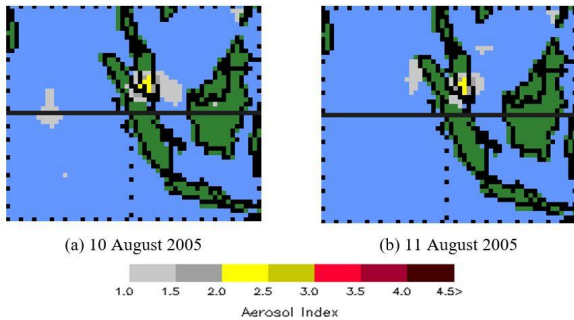


Figure 9: The aerosol index measured by the Total Ozone Mapping Spectrometer on (a) 10 and (b) 11 August 2005. The horizontal solid line and the vertical dashed line in the middle of the image represent latitude 0° and longitude 100° east respectively

In our study, visibility was used as the key parameter to describe haze severity. Air quality and visibility are measured at several stations by the Malaysian Meteorological Department. Here we display data from one of these stations, Petaling Jaya, in Selangor, Malaysia, to demonstrate haze occurrence and characteristics in Malaysia. Figure 10 shows a plot of daily visibility against day from 1999 to 2008. White, yellow, green, violet and red colours indicate clear (above 10 km visibility), moderate (5 – 10 km visibility), hazy (2 – 5 km visibility), very hazy (0.5 – 2 km visibility) and extremely hazy (less than 0.5 km visibility) conditions respectively. For most years, a drop in visibility can be observed at the end of the year, indicating the occurrence of severe haze.

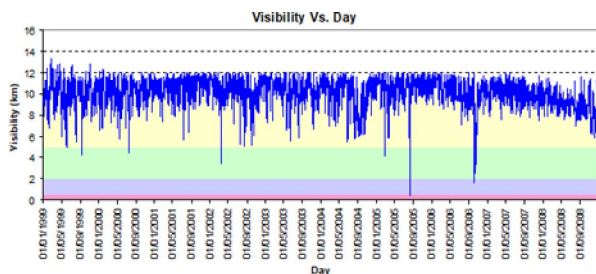


Figure 10: Visibility against day for Petaling Jaya from 1999 to 2008

Table 6 summarises the number of days for clear, moderate, hazy, very hazy and extremely hazy conditions in Petaling

Jaya from 1999 to 2008. The years which have the most days when the visibility is 10 km and less are 2008 (309), followed by 1999 (196), 2007 (159) and 2006 (156). To visualise the effects of haze, Figure 11 shows Landsat images of Bukit Beruntung in Selangor (approximately 30 km from Petaling Jaya) for (a) 6 August (5.8 km visibility) and (b) 22 August (11.7 km visibility) 2005; Landsat bands 3, 2 and 1 are assigned to red, green and blue respectively. For 6 August (Figure 11(a)), small patches of cloud and its shadow, masked in black, can be seen mainly on the top and left of the image, while haze covers mainly the middle and bottom parts of the image. Due to the haze, the distinction between different types of land cover is blurred, and their spectral signatures are altered. For 22 August (Figure 11(b)) the land cover can be recognised easily due to the clear conditions; bright areas represent urban, while dark areas, agricultural sites.

Table 6: Number of days for clear, moderate, hazy, very hazy, and extremely hazy conditions in Petaling Jaya from 1999 to 2008

Year	> 10 km (Clear)	5 to 10 (Moderate)	2 to 5 (Hazy)	500 to 2 (Very hazy)	< 0.5 km (Extremely hazy)
1999	179	184	2	0	0
2000	229	135	1	0	0
2001	265	100	0	0	0
2002	237	126	2	0	0
2003	234	131	0	0	0
2004	222	143	0	0	0
2005	259	101	3	1	1
2006	209	149	6	1	0
2007	206	159	0	0	0
2008	56	309	0	0	0

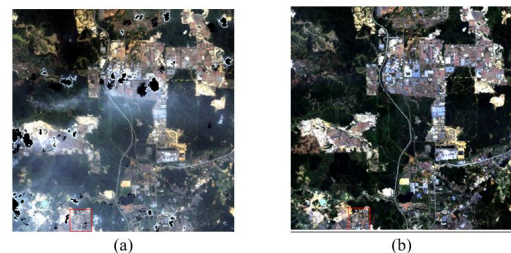


Figure 11: Landsat images of Bukit Beruntung acquired on (a) 6 August and (b) 22 August 2005, with bands 3, 2, 1 assigned to red, green and blue

Precision farming of paddy that requires continual near real-time data due to the fact that paddy needs approximately 120 days to grow before it can be harvested [20]. Satellite images have been the key inputs in monitoring its growth stages through satellite-derived vegetation indexes [21].

Figure 12 shows visibility against Landsat overpass date for 1999 to 2008. Landsat satellite overpasses Malaysia once every 16 days. For convenience, data with visibility 10 km and less are indicated by vertical bars. The red bars are data that overlap with the main paddy planting season (August to December), while the black bars show dates outside the planting season (January to July).

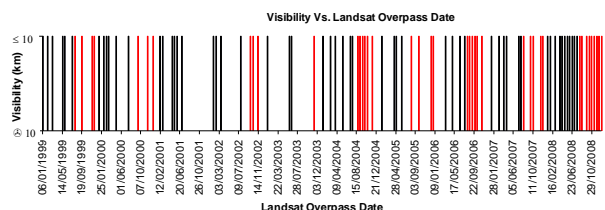


Figure 12: Visibility against Landsat overpass date in 2005 for Petaling Jaya. Black (off season) and red (main season) bars are Landsat data having visibility 10 km and less, no bar indicates data with visibility more than 10 km. The red bars are the haze affected data for the main planting season, while the black bars, for those outside the planting season

Table 7 summarises the number of Landsat overpass days overlapping with the main planting season (10 days) and having visibility 10 km and less, for Petaling Jaya from 1999 to 2008. Landsat gives 23 overpasses of the area each year, and 10 of them occur during the paddy main planting season. Out of these data, some of them have visibility 10 km and less, indicating that they were significantly affected by haze. 2008 has the most of haze-affected data (i.e. 9), followed by 2006 and 2004 (6), 2007 (5) and 2005 and 1999 (4). For other years, the number of days was 3 days and less. Consequently, for 2008, only one acquisition could be used during the main planting season, and only 4 for 2006 and 2004. 2007 (5) and 2005 and 1999 (6), have the most haze-free data. This shows that haze could hinder paddy monitoring using satellite images. Potential solutions to overcome such problem are implementing haze removal procedure or using different remote sensing platforms [22]. This includes unmanned aerial vehicles (UAVs) which can acquire images at low altitude and likely to lessen the haze effects [23], [24]. Effort to deal with haze issue is crucial to ensure continuous usability of remote sensing images not only for agriculture sectors but also others [25], [26]. These issues are even more critical to regions prone to be affected by sudden weather changes such as drop in atmospheric visibility due to volcano eruptions that produces large-scale volcanic ashes [27].

Table 7: Number of Landsat overpass days during the main planting season and the number having visibility 10 km and less, for Petaling Jaya from 1999 to 2008

Year	No. of overpasses overlapping with the main planting season and have visibility 10 km and less
1999	4
2000	3
2001	0
2002	3
2003	1
2004	6
2005	4
2006	6
2007	5
2008	9

4. CONCLUSION

The result shows within the period from 1999 to 2008, the 2008 paddy main planting season was the worst affected by haze where 9 out of 10 satellite overpasses occurred during the visibility conditions 10 km or less. Such situation could significantly hinder practices that require continual input from remote sensing images such as precision farming of paddy. Future study will investigate on images captured from drones for precision agriculture of paddy. Such images are captured at altitude less than 200 m and is likely to be less affected by haze and the same time capable of recording strong signal from ground. This could be an alternative to satellite images that can be easily degraded due to haze as concluded in this study.

ACKNOWLEDGEMENT

The authors thank Universiti Teknikal Malaysia Melaka (UTeM) for funding this research under the Ministry of Higher Education grant FRGS/2/2014/ICT02/UTEM/02/2 and the Malaysian Remote Sensing Agency for providing the remote sensing images.

REFERENCES

1. W. Morris. *The heritage illustrated dictionary of the English language*. Boston: American Heritage Publishing, 1975
2. M. Mahmud, M. Mesoscale equatorial wind prediction in Southeast Asia during a haze episode of 2005, *Geofizika*, vol. 26, no. 1, pp. 67 – 84. 2009.
3. C. Chiang, W. Chen, W. Liang, S. K. Das, and J. Nee. **Optical properties of tropospheric aerosols based on measurements of lidar, sun-photometer, and visibility at Chung-Li (251N, 1211E)**, *Atmospheric Environment*, vol. 41, pp. 4128 – 4137, 2007.

4. A. Ahmad and S. Quegan. **The effects of haze on the spectral and statistical properties of land cover classification**, *Applied Mathematical Sciences*, vol. 8, pp. 9001-9013, 2014.
<https://doi.org/10.12988/ams.2014.411939>
5. L. S. Guild, J. B. Kauffman, W. B. Cohen, C. A. Hlavka, and D. E. Ward. **Modelling biomass burning emissions for Amazon Forest and pastures in Rondônia, Brazil**, *Ecological Applications*, vol. 14, no. 4, pp. S232 – S246, 2004.
<https://doi.org/10.1890/01-6009>
6. M. Andreae, E. Browell, M. Garstang, G. Gregory, R. Harriss, G. Hill, D. Jacob, M. Pereira, G. Sachse, A. Setzer, D. Silva, R. Talbot, A. Torres, and S. Wofsey. **Biomass-burning emissions and associated haze layers over Amazonia**, *Journal of Geophysical Research*, vol. 93, no. D2, 1509 – 1527, 1988.
7. J. M. Haywood, J. Pelon, P. Formenti, N. Bharmal, M. E. Brooks, P. Capes, C. Chou, S. A. Christopher, H. Coe, J. Cuesta, Y. Derimian, K. Desboeufs, G. Greed, M. A. J. Harrison, B. Heese, E. J. Highwood, B. T. Johnson, T. M. Mallet, B. Marticorena, J. Marsham, S. F. Milton, G. Myhre, S. Osborne, D. J. Parker, J.-L. Rajot, M. Schulz, A. Slingo, D. Tanré, and P. Tulet. **Overview of the dust and biomass burning experiment and African monsoon multidisciplinary analysis special observing period**, *J. Geophysical Res.*, 113: D00C17, 2008.
8. C. O. Justice, J. D. Kendall, P. R. Dowty, and R. J. Scholes. **Satellite remote sensing of fires during SAFARI using the NOAA advanced very high-resolution radiometer**, *Journal of Geophysical Research*, 101: 23,851– 23,863, 1996.
9. D. Valero. *Fundamentals of Air Pollution*. San Diego, CA, USA: Elsevier Science, 2014.
10. W. T. Davis, T. Godish, and J. S. Fu. *Air Quality*. London: CRC Press, 2014.
11. A. Heil, B. Langmann, and E. Aldrian. **Indonesian peat and vegetation fire emissions: Study on factors influencing large-scale smoke haze pollution using a regional atmospheric chemistry model**, *Mitigation and Adaptation Strategies for Global Change*, vol. 12, no. 1, pp. 113 – 133, 2007.
12. R. Richter. **Classification metrics for improved atmospheric correction of multispectral VNIR imagery**, *Sensors*, vol. 8, pp. 6999 – 7011, 2008.
<https://doi.org/10.3390/s8116999>
13. Department of Environment Malaysia. *Kualiti Udara*. <https://www.doe.gov.my/portalv1/en/info-umum/kualiti-udara/114>, 2010.
14. Department of Environment. *Annual report 2004. Malaysia*: Department of Environment, 2004.
15. Department of Environment. *A guide to air pollution index (API) in Malaysia*. Malaysia: Department of Environment, 1997.
16. Henipavirus Ecology Collaborative Research Group (HERG). *Malaysia's smoke haze, 8th September 2005*. http://www.henipavirus.org/features/malaysia_smoke_haze/malaysia_smoke_haze.htm, 2010.
17. A. Ahmad and S. Quegan. **The effects of haze on the accuracy of satellite land cover classification**, *Applied Mathematical Sciences*, vol. 9, no. 49, pp. 2433-2443, 2015.
<https://doi.org/10.12988/ams.2015.52157>
18. The Star Online. **Open burning in Klang Valley banned**. <http://www.thestar.com.my/news/story.asp?file=/2005/8/9/nation/11717460&sec=nation>, 2005.
19. Ministry of Forestry Indonesia. **Ministry of Forestry Indonesia**. <http://www.dephut.go.id/index.php?q=en>, 2010.
20. G. Gupta and M. Nagar. **Agriculture sector in india: as a career**, *International Journal on Arts, Management and Humanities*, vol 6, no. 2, pp. 1 – 6, 2017.
21. R. Chaturvedi. **Data: The core of GIS**, *International Journal of Theoretical & Applied Sciences*, vol. 10, no. 1, pp. 34 – 39, 2018.
22. S. S. Rajpoot. **Image Enhancement Methods and Applications in Computational Photography**, *International Journal of Electrical, Electronics*, vol. 7, no. 2, pp. 91 – 97, 2018.
23. N. A. Sari, M. Y. A Sari, A. Ahmad, S. Sahib, and F. Othman. **Using LAPER Quadcopter Imagery for Precision Oil Palm Geospatial Intelligence (OP GeoInt)**, *Journal of Telecommunication, Electronic and Computer Engineering*, vol. 10, no. 1, pp. 25-33, 2018.
24. M. Y. A Sari, A. W. Rasib, K.M. Nazrin, A. Ahmad, N. A. Sari, D. Rozilawati, M.A. Hamzah and M.Y.A. Razak. **Terrain Mapping from Unmanned Aerial Vehicles**, *Journal of Advanced Manufacturing Technology*, vol. 13, no.1, pp.1-12, 2019.
25. P. Purwadi, N. Suryana, A. Nur, and B. Kusuma. **A comprehensive review: classification techniques on hyperspectral remote sensing**, *International Journal of Advanced Trends in Computer Science and Engineering*, vol. 8, pp. 156-164, 2019.
<https://doi.org/10.30534/ijatcse/2019/3181.52019>
26. D. Ahamad, M. Akhtar, and S. A. Hameed. **A review and analysis of big data and MapReduce**, *International Journal of Advanced Trends in Computer Science and Engineering*, vol. 8., pp. 1-3, 2019.
<https://doi.org/10.30534/ijatcse/2019/01812019>
27. C. Llorente. **Implementation of a web based weather monitoring station and data storage system**, *International Journal of Advanced Trends in Computer Science and Engineering*, vol. 8, pp. 527-530, 2019.
<https://doi.org/10.30534/ijatcse/2019/29832019>